

Content for Paper in English

- Special Events Using Traffic System Management Techniques.
EL-MEGEED.....
- Steel Fiber Reinforced Concrete Behaviour Under cyclic
.....
- HARA, E.S. KHALIFA, Y.H. HAMMAD**.....
tion of Radiated Petroleum resin on Sugar Cane Bagasse.
- MED, Z.A. NAGIEB, S.M. KAMAL**.....
asial Law for Steel Fiber Reinforced concrete.
- SHARA, E.S. KHALIFA, Y.H. HAMMAD**.....
st on the Skid Resistance Characteristics of Luminous Surfacing
- WISH**.....
Model Studies to Economize the Drainage System for Levees.
- AN, M.A. EL-SALAWY, A.M. EL-MOLLA**.....
ritical Flow on Riprap Stability.
- IAD, M.S. MOHAMED, E.A. ABDEL-HAFIEZ**.....
alysis of Vertical Underground Tanks.
- EG**.....
stem for Diermining the Construction Type of Buildings.
- W**.....
of Sewage Pipelines in Residential Areas Problems and Lessons.
- EG**.....
aviour of a Reinforced Concrete Cantilever Shear Wall.
- LAN**.....
ation of the Egyptian Geodetic Datum.
- KHEY**.....
ary Groundwater and Soil Studies on WADI EL-ASSIUTI by the
lite Images and GIS Techniques.
- AG, A.A. FARRAG**.....
t Analysis of GFRP Hop Contliver Beams.
- AHIM, H.N. ALY, I.G. SHAABAN, Y.A.ABD**
D.....

1094-1220

1021-1037

1038-105

1051-1072

1073-1083

1084-1092

1093-1106

1107-1119

1120-1131

1132-1145

1146-1160

1161-1184

1185-1205

1206-1225

FINITE ELEMENT ANALYSIS OF GFRP BOX CANTILEVER BEAMS**I. M. Ibrahim¹, H. N. Aly², I. G. Shaaban³ and Y. A. Abdel Megeed⁴**¹ Faculty of Engineering, Shoubra, Zagazig University-Banha Branch**ABSTRACT**

A finite element model was developed to trace the Static response of advanced composite thin walled beams made of Glass Fiber Reinforced Plastics (GFRP). The model is a four node rectangular layered element with six degrees of freedom per node. The element stiffness matrix for the model includes the effect of coupling between membrane and bending actions. The developed model has the capability of taking an arbitrary number of layers of different material properties for the analysis of a given section. To demonstrate the accuracy and convergence of the program, the results were compared with those obtained by others in the literature. Stable convergence and good accuracy were obtained. The effects of material anisotropy, fibers orientation, fiber volume fraction, coupling between membrane and bending actions and layers transposition on the deflection of thin-walled GFRP box cantilever beams were evaluated.

INTRODUCTION

Advanced composites or specifically fiber reinforced plastics (FRP) laminates are being increasingly used in structural applications. FRP composites are mainly made of reinforcing materials such as fiber glass, carbon fibers and aramid fibers and matrix (resin) materials such as thermosetting or thermoplastic materials [1]. The mechanical properties of composites vary significantly with the type and orientation of the constituent resins and fibers [2]. Compared to standard construction materials, composite materials present many advantages, e.g., light weight, corrosion resistance and electromagnetic transparency. Most prominent is the

tailoring the material for each particular application [3]. The high initial cost of composite materials is offset by their maintenance free performance. The low self-colored fiber reinforced polyester pultruded components offered many for the construction of light weight structures [4]. The design of structural manufactured from composite materials would initially involve the selection of the materials, fiber orientation, volume fraction of fibers in resin and manufacture for the composite, each item will have a particular influence upon the mechanical strength and stiffness of the final component [5]. To date, however, these have been rarely used in civil engineering structures in Egypt. This is probably the complexities arising from the nature and structure of these materials which analysis and design procedures [6].

FRP sections is normally based on the layered approach, which deals with the laminated composites where each lamina has a different orientation of fibers [7 and 8] methods for the analysis of thin plates and thin-walled beams made of laminated sections were developed earlier [9 and 10]. In this research, a rectangular element was used in order to study the theoretical behavior of advanced composite GFRP thin-walled beams. A parametric study was carried out using the developed finite element model in order to establish the influence of variation of moduli ratio (material anisotropy), fiber angle, fiber-volume fraction ratio, V_{f_1} , membrane-bending coupling and layers on the tip deflection of thin-walled GFRP box cantilever beams.

FORMATION OF A RECTANGULAR ELEMENT MODEL

Element Relations for GFRP Composite Sections

According to the classical lamination theory [11], the definite shape for composite material (multi-layered) section made up of several individual layers (laminae) in each layer the fibers are oriented in a matrix (see Figure 1). The strain-displacement relations at a distance z from the middle surface of the laminated composite section are

$$\epsilon = [u^0] + z [k] \quad (1)$$

$[e^0]$ contains the normal and shearing strains of the reference surface and, $[k]$ contains the changes in curvature and angle of twist of the reference surface during deformation.

$$[e^0] = \begin{bmatrix} \epsilon_x^0 \\ \epsilon_y^0 \\ \gamma_{xy}^0 \end{bmatrix} = \begin{bmatrix} \partial u / \partial x \\ \partial v / \partial y \\ \partial u / \partial y + \partial v / \partial x \end{bmatrix} \quad (2a)$$

and

$$[k] = \begin{bmatrix} k_x \\ k_y \\ k_{xy} \end{bmatrix} = \begin{bmatrix} \partial^2 w / \partial x^2 \\ \partial^2 w / \partial y^2 \\ 2(\partial^2 w / \partial x \partial y) \end{bmatrix} \quad (2b)$$

In which $(\partial u / \partial x, \partial v / \partial y, \dots)$ are the first derivatives of the tangential mid plane displacements, u, v, w is the deflection of the cross section and $(\partial^2 w / \partial x^2, \partial^2 w / \partial y^2, \dots)$ are the second order derivatives of the deflection, w .

Force-Deformation Relationship

Timoshenko, and Woinowsky-Krieger [12] reported that the resultant in-plane forces and bending moments for isotropic plates may be obtained by integration across the thickness of the plate (See Figure 2). By applying Hooke's law for the stress-strain relationship in two dimensional layered system [3] and substituting into Equation (2), the final form of the force deformation relationship of a composite section is written as:

$$\begin{bmatrix} [N] \\ [M] \end{bmatrix} = \begin{bmatrix} [A] & [B] \\ [B] & [D] \end{bmatrix} \begin{bmatrix} [e^0] \\ [k] \end{bmatrix} \quad (3)$$

Where

$[N]$ = Membrane forces matrix.

$[M]$ = Bending stress resultants.

$[A], [D]$ and $[B]$ are the effective membrane, bending and coupling stiffness matrices of a layered section, respectively.

derivation of the force-deformation relationship along with the matrices A, B, and D is elsewhere [3].

Element Formulation

A regular thin element of uniform thickness (t) with a local coordinates system o-x-y-z, o-x and o-y are paralleled to the sides of the element and positive z-direction is along z, is considered in the analysis. The origin is taken at the center of the element as shown in Figure 1. The degrees of freedom of each node are the in-plane displacements, u, v, the deflection, w, and the rotations θ_x , θ_y . The rotation, θ_z , was included to make the analysis of thin-walled sections of any shape more convenient.

The element stiffness matrix of advanced composite thin sections can be obtained through steps. Firstly by adding the contribution of membrane actions. Including the contribution of bending actions satisfies the second step. The last step deals with the coupling between membrane and bending actions.

Element Stiffness Matrix Due To Membrane Action

that the two displacement functions for u, v are first order polynomials as follows:

$$u = \alpha_1 + \alpha_2 x + \alpha_3 y + \alpha_4 xy \quad (4 a)$$

and

$$v = \alpha_5 + \alpha_6 x + \alpha_7 y + \alpha_8 xy \quad (4 b)$$

Equation 4 in a matrix form

$$[E] \{ \alpha \} \text{ and then, } \{ \alpha \} = [E]^{-1} \{ \delta \} \quad (5)$$

where $\{ \alpha \}$ is the vector of the unknown coefficients of the polynomials given in Equation (4) and can be expressed in terms of the u and v displacements of the nodes.

Equation (2 a) can be related at any point to displacements by differentiation and relation between strains and $\{ \alpha \}$ can be written in a matrix form as follows

$$\begin{bmatrix} \epsilon_x \\ \epsilon_y \\ \epsilon_{xy} \end{bmatrix} = \begin{bmatrix} \alpha_1 & \alpha_2 & \alpha_3 & \alpha_4 \\ \alpha_5 & \alpha_6 & \alpha_7 & \alpha_8 \\ \alpha_9 & \alpha_{10} & \alpha_{11} & \alpha_{12} \end{bmatrix} \begin{bmatrix} u \\ v \\ w \\ \theta_z \end{bmatrix}$$

Substituting Equation 5 into 6

$$\{ \epsilon \} = [C_p] \{ \delta \} \quad (7)$$

Where

$[C_p]$ = Strain-displacement matrix due to membrane action.

The relation between stresses and strains is

$$\begin{aligned} \{ \sigma \} &= [A] \{ \epsilon \} \\ \{ \sigma \} &= [A] [C_p] \{ \delta \} \end{aligned} \quad (8)$$

Applying the principle of virtual work to derive the element stiffness matrix by equating the internal work and the external work:

$$[K_p]_{8 \times 8} = t \int [C_p]^T [A] [C_p] ds \quad (9)$$

$[K_p]$ = element stiffness matrix due to membrane actions

ds = surface area of the element

2. Element Stiffness Matrix Due To Bending Action

Assuming that the displacement function is a third order polynomial function as follows:

$$w = \alpha_{10} x + \alpha_{11} y + \alpha_{12} z + \alpha_{13} xy + \alpha_{14} xz + \alpha_{15} yz + \alpha_{16} xyz + \alpha_{17} x^2 + \alpha_{18} x^2 y + \alpha_{19} x y^2 + \alpha_{20} y^2 + \alpha_{21} x^3 + \alpha_{22} x^2 y + \alpha_{23} xy^2 + \alpha_{24} y^3$$

Curvatures and twist in Equation (2 b) are related at any point to displacements by differentiating the displacement function, w, to the second order and then the curvature displacement matrix $[C_b]$ can be obtained in the same manner as in the membrane action.

$$[K_b]_{16 \times 16} = t \int [C_b]^T [D] [C_b] ds \quad (10)$$

Stiffness Matrix Due To Coupling Between Membrane And Bending Actions

Element stiffness matrix due to coupling is obtained as follows

$$[K_c]_{e,15} = t \int_s [C_b]^T [B] [C_p] ds \quad (11)$$

$$[K_c]_{e,15} = t \int_s [C_p]^T [D] [C_b] ds \quad (12)$$

At stiffness matrix due to coupling between membrane and bending actions

Energy of GFRP Advanced Composites

Energy of an anisotropic laminated element can be written as

$$\int_v \left\{ \begin{bmatrix} \{\epsilon^0\}^T [A] [B] \{\epsilon^0\} \\ \{k\}^T [B] [D] \{k\} \end{bmatrix} \right\} dv \quad (13 a)$$

Volume of the element

$$(13 b)$$

$\{\epsilon^0\}$ = The strain energy due to membrane action.

$\{k\}$ = The strain energy due to coupling between membrane and bending action.

$\{k, k\}$ = The strain energy due to bending action.

Equivalent Loads

Sum of the loads applied to the studied element can be expressed as

$$W = \int_s (X+Y+Z) ds \quad (14)$$

X , Y , and Z are the components of the loads applied to the studied element. The potential of a layered system is

The element stiffness matrix $[K]$ of order 24×24 can be obtained by applying the minimum total potential energy theorem. The full derivation of the element stiffness matrix is detailed elsewhere [3].

Transformation of Coordinates

The transformation matrix $[\lambda]$ between the local and global coordinates systems shall be derived in order to analyze thin walled sections of any shape. The relationship between the displacements in local and global systems at node i of a typical element, shown in Figure 4, may be written in a matrix form as

$$\begin{bmatrix} u_i \\ v_i \\ w_i \\ \theta_{x_i} \\ \theta_{y_i} \\ \theta_{z_i} \end{bmatrix} = \begin{bmatrix} 1 & 0 & 0 & 0 & 0 & 0 \\ 0 & \cos \beta & \sin \beta & 0 & 0 & 0 \\ 0 & -\sin \beta & \cos \beta & 0 & 0 & 0 \\ 0 & 0 & 0 & 1 & 0 & 0 \\ 0 & 0 & 0 & 0 & \cos \beta & \sin \beta \\ 0 & 0 & 0 & 0 & -\sin \beta & \cos \beta \end{bmatrix} \begin{bmatrix} \bar{u}_i \\ \bar{v}_i \\ \bar{w}_i \\ \bar{\theta}_{x_i} \\ \bar{\theta}_{y_i} \\ \bar{\theta}_{z_i} \end{bmatrix} \quad (16)$$

In which $u, v, w, \theta_x, \theta_y, \theta_z$ = the reference surface displacements components of node i in the x, y, z direction, respectively, and $\bar{u}, \bar{v}, \bar{w}, \bar{\theta}_x, \bar{\theta}_y, \bar{\theta}_z$ = the corresponding displacements in the X, Y, Z direction. Equation (16) can be summarized as

$$[\delta] = [R][\bar{\delta}]$$

Applying the transformation matrix for the four nodes element, the element transformation matrix $[\lambda]_{15,24}$ can be obtained and then the element stiffness matrix $[\bar{K}]_{15,24}$ can be assembled in the global coordinate system.

$$[\bar{K}] = [\lambda]^T [K] [\lambda] \quad (17)$$

EVALUATIVE ANALYSIS

The finite element formulation has been evaluated by analyzing the following problems. The first problem aims to check the accuracy of the model while the other problems show the

An isotropic thin-walled box section cantilever beam of length = 60" (152.4 cm), width = 18" (45.72 cm) and height = 12" (30.48 cm) - see Figure 5 - was analyzed using the developed model in order to check its accuracy. Tip load $P = 5000$ lb (2.3 ton) was applied at each corner of the beam, as shown in Figure 5. Modulus of elasticity for the material of this beam was 30×10^6 psi (2109.26 t/cm²) and Poisson's ratio, $\nu = 0.25$. The finite element idealization consists of 24 nodes, and 20 elements. The degrees of freedom of each node equal six degrees of freedom, and the total degrees of freedom of the structure is $20 \times 6 = 120$. The tip deflection predicted by the proposed numerical model was compared with that obtained by the simple beam theory [13]. The predicted tip deflection was 0.0216105" (0.0548906 cm) and that obtained by applying the simple beam theory [13] was 0.0204" (0.051816 cm). It is clear that the developed model gives an excellent agreement with the simple beam theory applied by Timoshenko and Goodier [13]. The behavior of some other structures was predicted successfully by the developed model and the results are detailed elsewhere [3].

Effect of Material Anisotropy (Moduli Ratio, E_{11} / E_{22})

A cantilever GFRP composite box section beam of length = 180 cm and breadth $B =$ Height $H = 20$ cm was analyzed in order to assess the effect of changing moduli ratio for the material of such thin-walled section. The thickness of the beam section equals 1 cm and consists of three GFRP layers of fiber orientations ($0^\circ / 90^\circ / 0^\circ$) of equal thickness. The beam was subjected to a load of 1.5 ton at the tip (0.75 ton at each corner). The material properties of the GFRP beams were as follows:

$$E_{11} / E_{22} \text{ had variable ratios} = 2, 5, 10, 20, 30, 40, 50, \quad G_{12} / E_{22} = 0.5, \quad \nu_{12} = 0.25$$

Where

$$E_{22} = 70.5 \text{ t/cm}^2$$

E = Modulus of elasticity, G = Shear modulus, ν = Poisson's ratio

The subscripts (1) and (2) refer to the longitudinal and transverse directions of fibers respectively (See Figure 1).

Figure 6 shows the deflection results versus different ratios of E_{11} / E_{22} in a graphical form. It can be seen that an increase in the moduli ratio results in a significant decrease in the

deflection from 4.1 cm to 0.42 cm. This behavior may be attributed to the stiffness of the studied section increases with an increase in the material anisotropy ratio. This is in agreement with the expected behavior of the beam since a high ratio indicative of higher modulus of elasticity in the longitudinal direction along which straining actions are exhibited. It is to be noted that an increase of the modulus ratio value of about 25 provides very limited enhancement in the beam deflection.

Effect of Fibers Orientation Angle

The cantilever beam, studied above, was reanalyzed to assess the effect of fiber orientation angle of the layers of such thin-walled box section on its behavior. The section of the beam is of the same thickness and properties as in the previous problem cases were studied in this problem, the first one is a control case of top, bottom two webs with lay up of ($0^\circ / 90^\circ / 0^\circ$). The second case had orientation angles (0° for the two webs and different orientation angles ($0^\circ / 90^\circ / 0^\circ$) for top and bottom flanges). The third one kept the orientation angles ($0^\circ / 90^\circ / 0^\circ$) for the top and bottom flanges and the two webs had different orientation angles ($0^\circ / \theta^\circ / 0^\circ$). The last case considered fibers orientation angles are different ($0^\circ / \theta^\circ / 0^\circ$) for all four sides of the section, orientation angles were $\theta^\circ = 15^\circ, 25^\circ, 35^\circ$ and 45° . The material properties of beams were as follows:

$$E_{11} / E_{22} = 40,$$

$$G_{12} / E_{22} = 0.5,$$

Where

$$E_{11} = 2820 \text{ t/cm}^2 \text{ and } E_{22} = 70.5 \text{ t/cm}^2$$

The deflection results for different fibers orientation angles are shown in Figure 7 as expected, the control case, i.e. Case 1 showed no variation in deflections as orientations varied. Case 2 was shown to be the closest to the results of Case 1 as deflections tended to increase slightly with an increase in the angle of orientation. Cases, deflection values on the order of 0.47cm were noted. Cases 3 and 4, on the other hand, provided the better deflection results where both cases shared a common optimum fiber orientation that was in the vicinity of 30° . At the optimum angle, the beams

near values of tip deflections, namely 0.3 cm. Thus, cases 1 and 2 yielded 50% more deflection compared to cases 3 and 4. It can be argued that the contribution of the webs to the stiffness of the beam section is more than the contribution of top and bottom flanges. Cases 3 and 4 had lower deflection for the fibers oriented closer to the longitudinal axis of the beam compared with Cases 1 and 2.

Effect of Fiber Volume Fraction

In the previous section, the fiber-volume fraction of the four sides of the thin-walled box section beam was varied as a variable instead of the fibers orientation angle. The change of fiber volume fraction, in turn, affected the material properties as presented in Table 1 [14]. The fibers orientation angle for the box-section beam was kept constant of lay up ($0^\circ / 90^\circ / 0^\circ$). The fibers studied previously were reanalyzed in order to assess the effect of fiber volume fraction on the behavior of thin-walled beams. The first case is considered as a control case, with material properties as in the previously studied beam. The second one had the same material properties for the two webs and five different material sets of variable fiber volume fraction were considered for the top and bottom flanges. The proposed material sets were taken from Ref. [14] and presented in Table 1. In the third case, the material properties were kept constant for the top and bottom flanges while the two webs had the five different material sets shown in Table 1. The fourth and last case considered that the five different material sets

from Table 1 are applied to all four sides of the section.

The numerical results for tip deflection are shown in Figure 8. It can be seen from the figure that case 4 is the most one affected by changing the fiber-volume fraction. For example, the tip deflection of fiber volume fraction from 27% (material set 1) to 64% (material set 5) resulted in a deflection of 0.35 cm to 0.17 cm. Moreover, Figure 8 shows that cases 2 and 3 were affected by the fiber-volume fraction more than their sensitivity to the change in fiber orientation angle (see Figure 7). It is interesting to notice that the deflection values obtained for fibers orientation angle to 25° for Case 2 and between 25° - 35° for Cases 3 and 4 were very close to those obtained by increasing the fiber-volume fraction to material Set 2) as shown in Figure 8. However, it should be noted that it is more difficult to adjust fiber orientations than to increase the fiber-volume fraction.

Effect of Coupling between Membrane and Bending Actions. In the previously studied beams, the box-section was considered to consist of three symmetric layers of equal thickness. This leads to a balanced section with negligible coupling between membrane and bending actions. In order to study the effect of such coupling on the behavior of the studied box-section beam, the section was considered to be of the same thickness (1.0 cm) but to consist of two cross ply layers ($0^\circ / 90^\circ$) of equal thickness. The coupling effect was assessed by comparing the deflection results for different moduli ratios to those obtained by neglecting the coupling between membrane and bending actions, i.e. omitting the [B] matrix in Equation (13) from the element stiffness matrix. Figure 9 shows the results of the two cases along with the results of three layers ($0^\circ / 90^\circ / 0^\circ$) shown in Figure 6. It can be seen from the figure that neglecting the coupling effect leads to an underestimation of the deflection results, which may, in turn, lead to a misleading approach for the design of such elements. However, the coupling effect vanishes with the decrease of moduli ratio. It is interesting to notice that the results of 3 symmetric layers ($0^\circ / 90^\circ / 0^\circ$) are close to those of cross ply layers ($0^\circ / 90^\circ$) after neglecting coupling (orthotropic solution). This is probably due to the absence of coupling in the case of three (odd number) of symmetric layers. This condition is in essence analogous to forcing a beam where coupling is inherent to behave as though such coupling does not exist.

Effect of Layer Transposition

Figure 10 depicts the effect of layer transposition on the tip deflection for a range of moduli ratios. The basic trend of deflection reduction along with an increase in the moduli ratio remains evident, however, beams with $90^\circ / 0^\circ / 90^\circ$ arrangement are observed to yield higher deflections as compared to identical beams with $0^\circ / 90^\circ / 0^\circ$ arrangement. This result signifies that longitudinal membrane action is predominant to transverse membrane action since the composite parameters of these cases are obtained by interchanging A_{11} and A_{22} with the remaining terms being the same. This is in agreement with the expected beam behavior where longitudinal stresses are predominant to transverse stresses.

In the case of angle ply arrangement, the above mentioned trend consistently prevails as may be seen in Figure 11 (a) through (d). A notable distinction in this figure, however, is that Case 1 (control) and Case 2 were the most affected by layer transposition. The layer transposition

increases with the increase of fiber orientation angle especially for Case 2. For example, effect of layer transposition increased the deflection values for Case 2 by 27%, 33%, 36% and 37% for fiber orientation angles of 15°, 25°, 35° and 45°, respectively. Despite the fact, Cases 3 and 4 had lower deflection values than Cases 1 and 2, as explained above, they had less sensitivity to layer transposition.

Fig. 2 presents the effect of layer transposition on the deflection for various percentages of volume fraction. Notable differences in the values of deflections were observed. For an increase of about 36% in the deflection is detected with all five material sets having the same deflection magnitudes. For Case 2, the increase is in the order of 28%, and for Case 3 it is about 40% versus 30% for Case 4. A valuable observation for cases 2 and 3 is that deflections tend to decrease with an increase in the percentage of fiber fraction.

CONCLUSIONS

From the scope of this investigation, the following conclusions may be drawn:

The finite element model developed in this paper is capable of predicting the behavior of thin-walled beams in an accurate and efficient manner. The formulation included in the paper can be easily linked to any ready package thus providing a valuable numerical module for the analysis of a broad spectrum of related GFRP beam problems. Increasing the moduli ratio (material anisotropy) leads to a great increase in the stiffness of thin-walled GFRP beams of moduli ratios up to about 25, such an increase, however, is insignificant for higher ratios. Within the scope of this work, a moduli ratio of 25 is considered an optimum choice.

Both of the fiber orientation angle and fiber volume fraction lead to a decrease in the deflection of the studied advanced composite thin-walled beams. However, increasing the fiber volume fraction is more costly than increasing the angle of fiber orientation.

The interaction between membrane and bending actions softens the beam's resistance. Thus the effect of coupling is to reduce the effective stiffness of the studied section. The degree of such reduction depends on the degree of material anisotropy (moduli ratio). It

is, therefore, recommended that judicious choice of fiber patterns be made in order to avoid such coupling whenever possible.

5. Layer transposition has an impact on deflection for those beams possessing extreme values of percentage of fiber volume fraction, i.e., highest and lowest, whereas beams possessing moderate volume fractions are insensitive to such a transposition.
6. Deflections consistently decreased when fibers are oriented closer to the longitudinal axis of the beam. This behavior remains unchanged for cross-ply laminates as well as angle-ply laminates.

REFERENCES

1. Bishop, W. J., "Advanced Composites." Copy right by Ivana, K. P. Elsevier. Science Publisher LTD. Crown House, Linton Road, Barking. Essex. IIGI 8JU, England, 1989.
2. Basumaty, H. "Fiber Composites for New and Existing Structures", ACI Structural Journal, Vol. 91, No. 3, May-June 1994, pp. 346-354.
3. Abdel-mageed, Y. A., "Static Response of Fiber Reinforced Polymer Pultruded Structures" M.Sc. thesis submitted to Zagazig University, Bahja Branch, 1997.
4. Harvey, W. J., "A Reinforced Plastic Footbridge" Aberfeldy, U. K., Structural Engineering Internationally, No. 4, 1993.
5. Phillips, L. N., "Design With Advanced Composite Materials" The design Council, Haymarket, London SW1Y 4SU, 1989.
6. Mallick, P. K., "Fiber-reinforced composites: Materials, Manufacturing, and Design" Marcel Dekker Inc., New York, 1988, pp. 145-165.
7. Ibrahim, I. M. and Shaaban, I. G., "Analysis and Behavior of FRP Composites for New and Existing Structures", State-of-the-Art Report, The first Middle East Workshop Structural Composites, Sharm El-sheikh, Egypt, June 1996, pp. 147-160.
8. Basanapur, A. G., "Method Of Analysis For Advanced Composite Structures" Advanced Composites Materials In Civil Engineering Structures, Ed. S.L. Iyer and R. Sen, A.S.C. 1991, pp. 316-347.
9. Aly, H. N. and Shaaban, I. G., "Analysis Of Skew Composite Plates" Civil Engineering Research Magazine, Al-Azhar University, Vol. 16, No. 7, 1994, pp. 616-631.

11 Ashton, J. E., Halpin, J. C., and Petit, P. H., "Primer On Composite Materials: Analysis" Technomic Publishing Co., Stamford, Conn., 1969

12 Timoshenko, S. P. and Woinowsky-Krieger, S., "Theory Of Plates And Shells", 2nd ed. McGraw-Hill Book Co., Inc., New York, 1959

13 Timoshenko, S. P. and Goodier, J. N., "Theory of Elasticity, 3rd Edn. McGraw-Hill, New York, 1970

14 Dimitrios, K., "A Simple and Efficient Curved Beam Element for the Linear and Non-linear Analysis of Laminated Composite Structures", Computers and Structures, Vol. 29, No. 4, 1988, pp. 623-632

Table 1 Material properties of unidirectionally glass-reinforced materials [14]

Material no	% of fiber volume fraction	E_{11} (t/cm ²)	E_{22} (t/cm ²)	G_{12} (t/cm ²)	ν_{12}
1	27	2190	434	161	0.31
2	39	3020	513	190	0.29
3	46	3504	575	213	0.28
4	57	4565	707	263	0.26
5	64	4750	429	399	0.25

Table 2 Effect of layer transposition and fiber volume fraction on the deflection of the studied box cantilever beam.

Material	Case 1 (Control)		Case 2		Case 3		Case 4	
	0° / 90° / 0°	90° / 0° / 90°	0° / 90° / 0°	90° / 0° / 90°	0° / 90° / 0°	90° / 0° / 90°	0° / 90° / 0°	90° / 0° / 90°
1	0.47	0.73	0.51	0.71	0.32	0.54	0.36	0.52
2	0.47	0.73	0.46	0.64	0.30	0.50	0.30	0.43
3	0.47	0.73	0.41	0.57	0.28	0.46	0.24	0.35
4	0.47	0.73	0.38	0.52	0.26	0.42	0.20	0.31
5	0.47	0.73	0.36	0.48	0.24	0.39	0.17	0.26

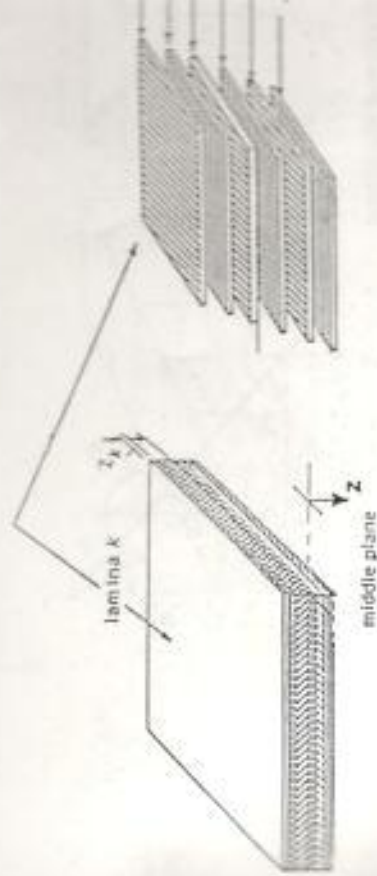


Figure 1 A typical advanced composite section with lamina of different orientations

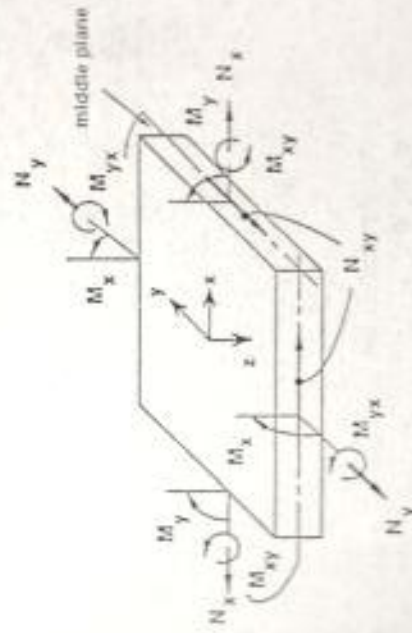


Figure 2 Stress resultants applied to a laminated advanced composite section

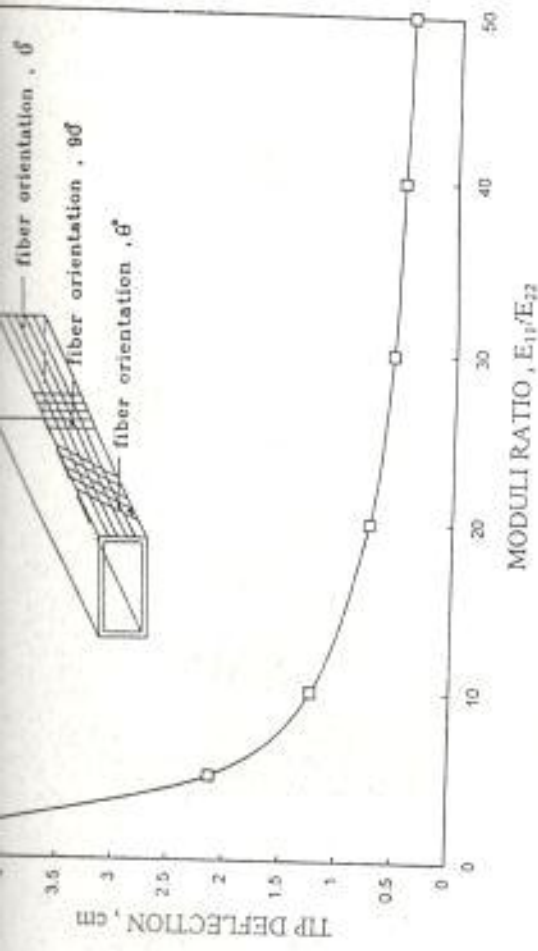


Figure 6 Effect of material anisotropy on the deflection of GFRP box cantilever beam.

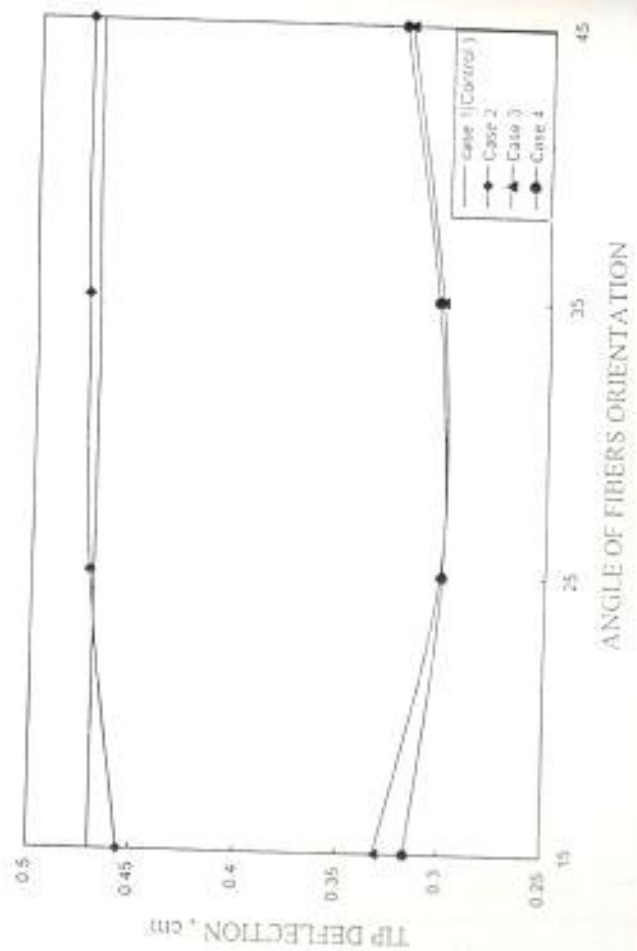


Figure 7 Effect of fibers orientation angle on the tip deflection of GFRP composite box-section beam.

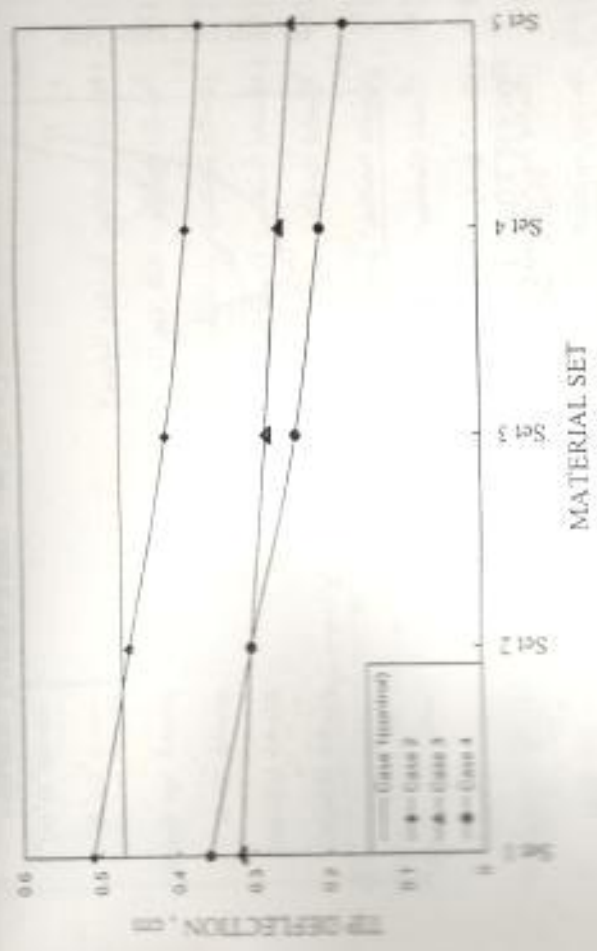


Figure 8 Effect of fiber-volume fraction on the tip deflection of GFRP box-section beam.

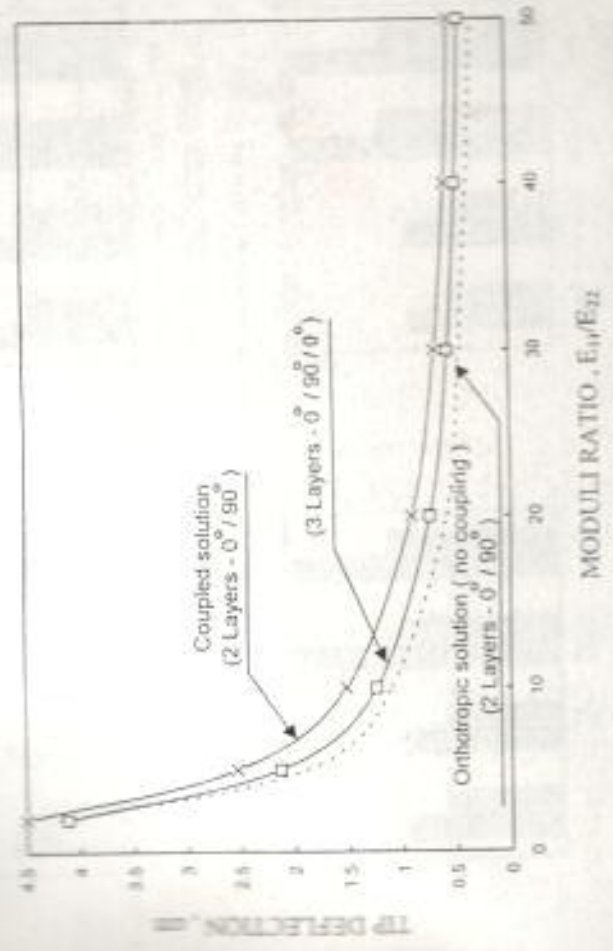


Figure 9 Effect of coupling on the behavior of box-section beam for different moduli ratios.

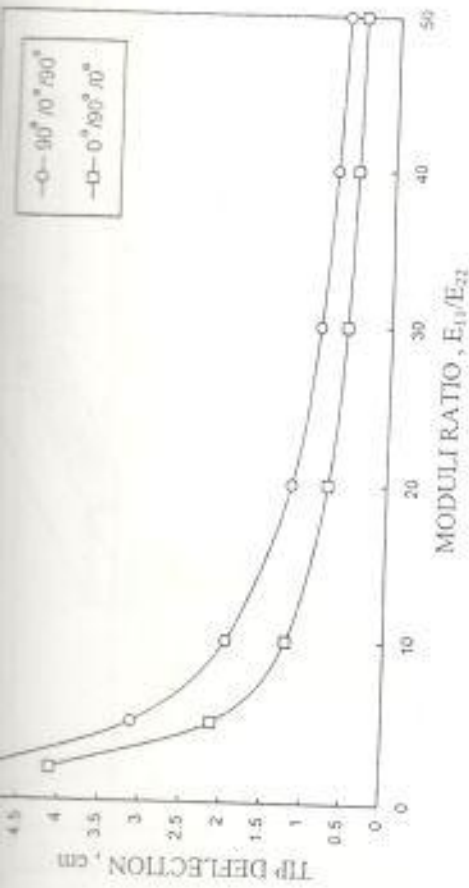
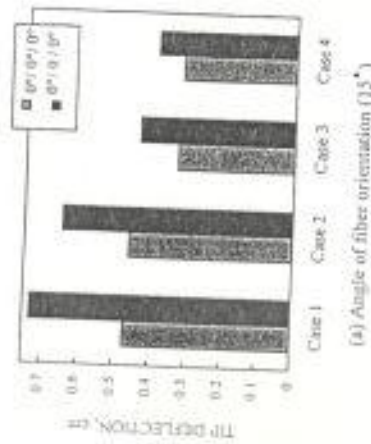
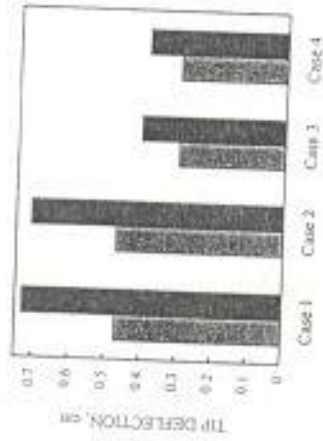


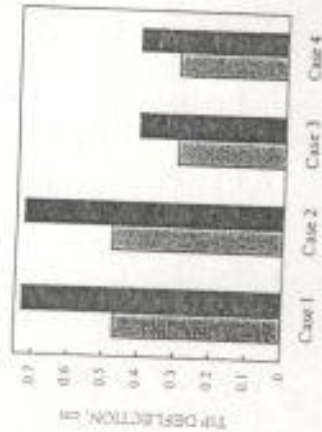
Figure 10 Effect of layers transposition on the deflection of GFRP box-section beam for different moduli ratios.



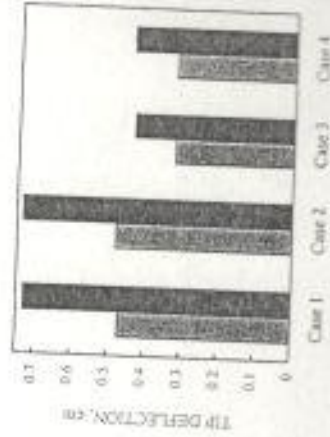
(a) Angle of fiber orientation (15°)



(b) Angle of fiber orientation (25°)



(c) Angle of fiber orientation (35°)

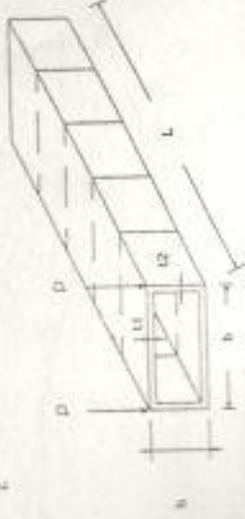


(d) Angle of fiber orientation (45°)

Figure 11 Effect of layers transposition on the deflection of the studied beam for different fiber orientations.

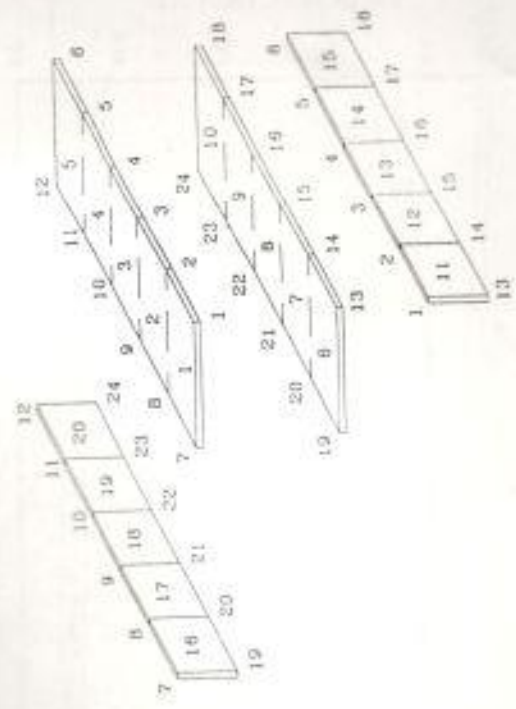
جامعة عين شمس
جامعة عين شمس
جامعة الأزهر
جامعة المنصورة
جامعة المنوفية
جامعة الأزهر
مركز بحوث البناء
جامعة القاهرة
جامعة القاهرة
جامعة الأزهر
جامعة عين شمس
جامعة القاهرة
جامعة القاهرة
جامعة الأزهر
جامعة القاهرة
جامعة القاهرة
جامعة الأزهر
جامعة عين شمس
جامعة الأزهر

الأستاذ الدكتور / إبراهيم المصري (١)
الأستاذ الدكتور / علي أبو العباس (٢)
الأستاذ الدكتور / جمال شريف (٣)
الأستاذ الدكتور / أحمد حسنين عبد الرحيم (٤)
الأستاذ الدكتور / منير محمد كمال (٥)
الأستاذ الدكتور / محمود أحمد مطاوع (٦)
الأستاذ الدكتور / حمد حامد شاهين (٧)
الأستاذ الدكتور / أحمد عاطف جاد الله (٨)
الأستاذ الدكتور / ليلى صلاح الدين رضوان (٩)
الأستاذ الدكتور / محمد الفريب حامد (١٠)
الأستاذ الدكتور / محمد البازي جهاد (١١)
الأستاذ الدكتور / عبد الرحمن صادق بازوغ (١٢)
الأستاذ الدكتور / مصطفى كامل الفهداوي (١٣)
الأستاذ الدكتور / أحمد رجب (١٤)
الأستاذ الدكتور / علي عبد الرحمن (١٥)
الأستاذ الدكتور / محمد شوقي الفرزالي (١٦)
الأستاذ الدكتور / محمود النقراشي عثمان (١٧)
الأستاذ الدكتور / محمد محمد نهار (١٨)
الأستاذ الدكتور / عصام قنار (١٩)



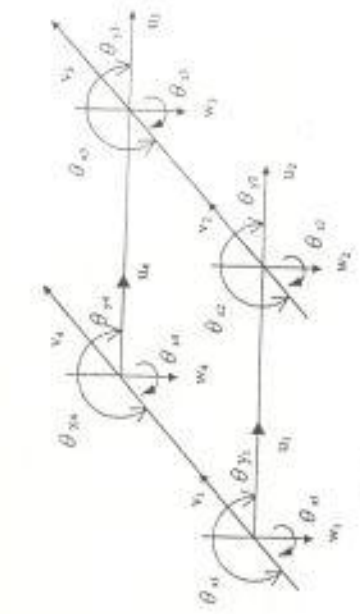
- t1 = 1.0 inch (2.54 cm)
- t2 = 0.5 inch (1.27 cm)
- b = 18 inch (45.72 cm)
- h = 12 inch (30.48 cm)

(a) Dimensions, loading conditions and mesh distribution.



(b) Node and element numbering scheme

Figure 5. Finite element idealization of a box-section isotropic beam



(b) In-plane and normal displacements

Figure 3. A rectangular element with six degrees of freedom per node

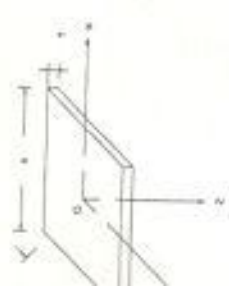


Figure 4. Individual and common coordinate systems

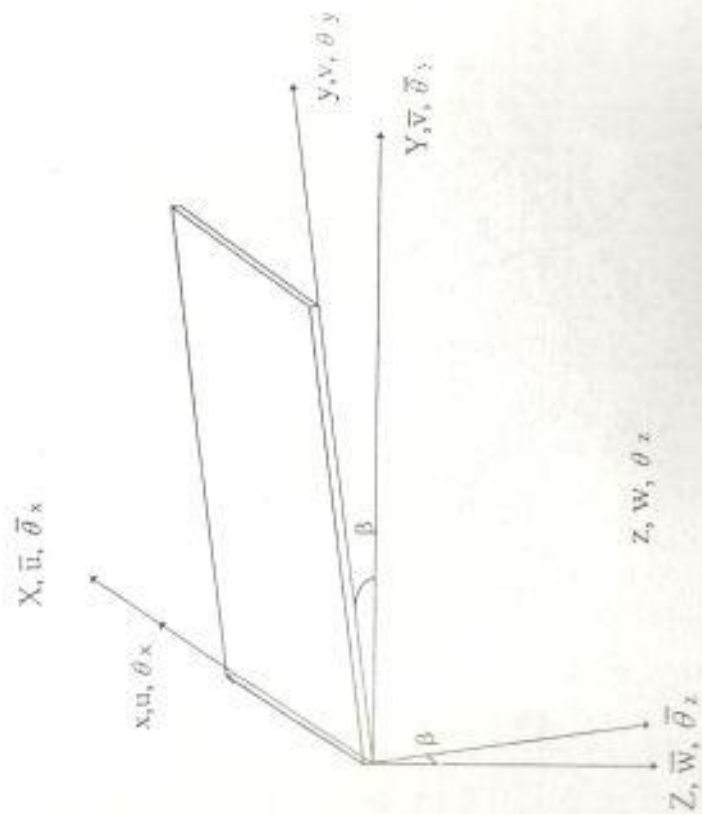


Figure 4. Individual and common coordinate systems